Grant Agreement Number:
641185

Action acronym:
CEMCAP

Action full title:
CO₂ capture from cement production

Type of action:

H2020-LCE-2014-2015/H2020-LCE-2014-1

Starting date of the action: 2015-05-01
Duration: 42 months

D4.1
Design and performance of CEMCAP cement plant without CO₂ capture

Due delivery date: 2016-04-30
Actual delivery date: 2016-05-04

Organization name of lead participant for this deliverable:
Politecnico di Milano

Project co-funded by the European Commission within Horizon2020		
Dissemination Level		
PU	Public	X
CO	Confidential , only for members of the consortium (including the Commission Services)	

Deliverable number:	D4.1
Deliverable title:	Design and performance of CEMCAP cement plant without CO_2 capture
Work package:	WP4: Comparative capture process analysis
Lead participant:	SINTEF ER

Authors		
Name	**Organisation**	**E-mail**
Stefano Campanari	Politecnico di Milano	stefano.campanari@polimi.it
Giovanni Cinti	Italcementi	g.cinti@itcgr.net
Stefano Consonni	Politecnico di Milano	stefano.consonni@polimi.it
Kristina Fleiger	VDZ gGmbH	kristina.fleiger@vdz-online.de
Manuele Gatti	Politecnico di Milano	manuele.gatti@polimi.it
Helmut Hoppe	VDZ gGmbH	helmut.hoppe@vdz-online.de
Isabel Martínez	Politecnico di Milano	isabel.martinez@polimi.it
Matteo Romano	Politecnico di Milano	matteo.romano@polimi.it
Maurizio Spinelli	Politecnico di Milano	maurizio.spinelli@polimi.it
Mari Voldsund	SINTEF ER	Mari.Voldsund@sintef.no

Abstract

In this deliverable, the mass and energy balances of the benchmark cement plant without CO_2 capture are presented. The balances have been derived from a VDZ model developed in previous projects and reproduced by Politecnico di Milano.

The electric consumptions of the benchmark plant have also been defined, focusing on the consumptions of the fans that may change when integration of CO_2 capture technologies is considered.

In the final section, the economic analysis of the reference cement plant is also presented, defining the industrial cost of cement. A sensitivity analysis on the effect of fuel and electricity prices and of a carbon tax is also included.

TABLE OF CONTENTS

List of abbreviations

COC	Cost of cement
CT	Carbon tax
EPC	Engineering, Procurement and Construction Costs
POE	Price of electricity
TDC	Total Direct Costs
TPC	Total Plant Costs

1   INTRODUCTION

The aim of this deliverable is to present the process models used for the simulation of the reference clinker burning line without CO_2 capture and the economic analysis of the associated cement plant.

The initial model of the benchmark cement kiln has been developed by VDZ in past projects and used as reference in previous ECRA reports [ECRA]. In CEMCAP, the mass and energy balances of this reference cement kiln have been reproduced by Politecnico di Milano (Polimi) with a simplified process modelling approach, by means of the in-house process modelling code GS. This model calibration is necessary in order to have consistent and comparable results of the CO_2 capture processes involving the modification of the cement kiln. In CEMCAP, this is relevant for the oxyfuel and the Calcium looping technologies, which will be evaluated by VDZ and Polimi respectively.

In addition to cement kiln model calibration, the share of the electric consumption is defined, with specific attention to the consumption of fans, that may change from case to case when CO_2 capture technologies are considered.

Finally, in the last section, the economic analysis of the benchmark cement plant is presented, including a sensitivity analysis on the fuel price, electricity price and carbon tax.

2 REFERENCE CEMENT PLANT WITHOUT CO$_2$ CAPTURE

The CEMCAP reference cement plant without CO$_2$ capture is based on the Best Available Technique (BAT) standard as defined in the European BREF-Document (Best Available Technique Reference) for the manufacture of cement [BREF, 2013]. The process configuration of the reference cement kiln, based on a dry kiln process, consists of a five stage cyclone preheater, a calciner with tertiary duct, a rotary kiln and a grate cooler, as illustrated in Figure 2.1. This case is used as reference also in the ECRA project, and a process model of the plant has previously been built by VDZ.

The plant is described in CEMCAP deliverable 3.2 "CEMCAP framework for comparative techno-economic analysis of CO$_2$ capture from cement plants" and is briefly described in this section for completeness.
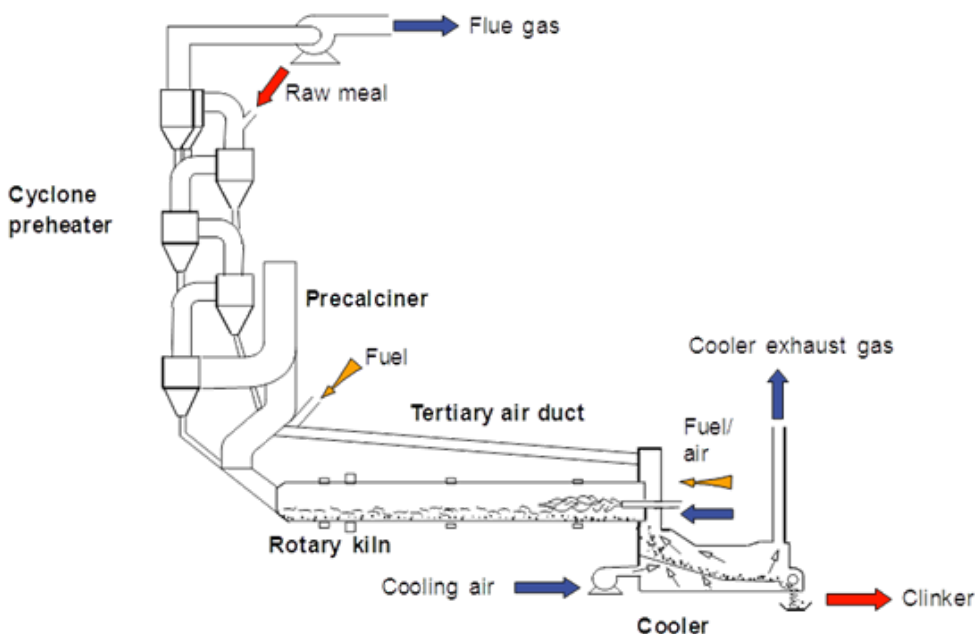

Figure 2.1: Configuration of the reference cement kiln without CO$_2$ capture.

The plant has a clinker capacity of about 3000 t/d (raw meal/clinker factor 1.6), which is a representative size for a European cement plant. This corresponds to a yearly clinker production of 1 Mt (equivalent to a run time of >330 days per year) or a cement production of 1.36 Mt per year (clinker/cement factor 0.737).

The cyclone preheater consists of five cyclone stages arranged above one another. The raw meal (kiln feed) passes through the process stages of preheating and calcining in succession from top to bottom before reaching the rotary kiln. The flow of process gases is essentially counter to the flow of the kiln feed. Each cyclone stage is made of two parts: the connecting duct which connects each cyclone to the one above, where the material and gas phase are in direct contact with each other allowing an extensive heat transfer, and the cyclone itself, where the raw meal is separated from the flue gas due to centrifugal forces.

Calcination, which is the decomposition of calcium carbonate to calcium oxide and CO$_2$, is carried out in the calciner, where 62% of the total plant fuel input is consumed. The calciner has an in-line

design with tertiary air duct providing hot tertiary air from the clinker cooler. A calcination level of about 94% is achieved in the calciner.

The completion of calcination, the formation of the clinker phases and the granulation of the kiln charge take place in the rotary kiln. The rotary kiln represents therefore the core of the burning process. Rotary kilns are steel tubes, placed on 2 or 3 roller stations, inclined between 3% and 4% towards the discharge end, rotating at a rate of about 1.3 to 3.5 revolutions per minute. The length of the kiln depends on production capacity and the extent of calcination of the raw meal entering the rotary kiln. Modern rotary kilns with preheater and calciner are 50 m to 80 m long and have a diameter between three and seven meters. The inside of the rotary kiln is lined with refractory bricks as the high temperatures in the kiln (gas phase up to 2,000°C, material 1,450°C) would otherwise destroy the tube. Depending on the length of the kiln the gas residence time is 2 to 4 seconds at temperatures greater than 1,200°C. The solid material takes 20 to 40 minutes to pass through the kiln depending on the degree of calcination and the size of the kiln. During its way through the kiln the raw material components form the mineralogical phases via intermediate phases.

The hot clinker is discharged from the kiln to a grate cooler. Here, cooling air flows through it from below, according to a cross flow heat exchange mechanism. The cooler generates the secondary combustion air, which flows through the kiln hood to the rotary kiln, and the tertiary combustion air, which flows through a connection located on the hot part of the cooler or in the kiln hood and then along the tertiary air duct up to the calciner.

3 REFERENCE CEMENT PLANT MODELLING

3.1 VDZ model

The process model previously developed by VDZ was used as basis for the definition of the reference cement kiln model developed by Polimi in this work.

At its core the VDZ model describes the process from the kiln meal feed to the discharge of the clinker from the cooler and is made up of individual models for the plant components preheater, calciner, bypass, rotary kiln and grate cooler. It is also possible to incorporate the plant sections of the external cycle, i.e. the evaporative cooler, raw grinding plant and dust collector. All the individual models can be linked mathematically with one another, which makes it possible to determine a steady-state condition for the entire rotary kiln plant. Because of the modular structure the different plant circuits can be mathematically simulated comparatively easily and flexibly (Figure 3.1). The individual plant sections can also be defined geometrically so that different plant sizes can be simulated. Further, inputs relate to the composition and mass flows of the raw materials and fuels as well as the volumetric flows of cooler inlet air, secondary air and, where appropriate, tertiary air.
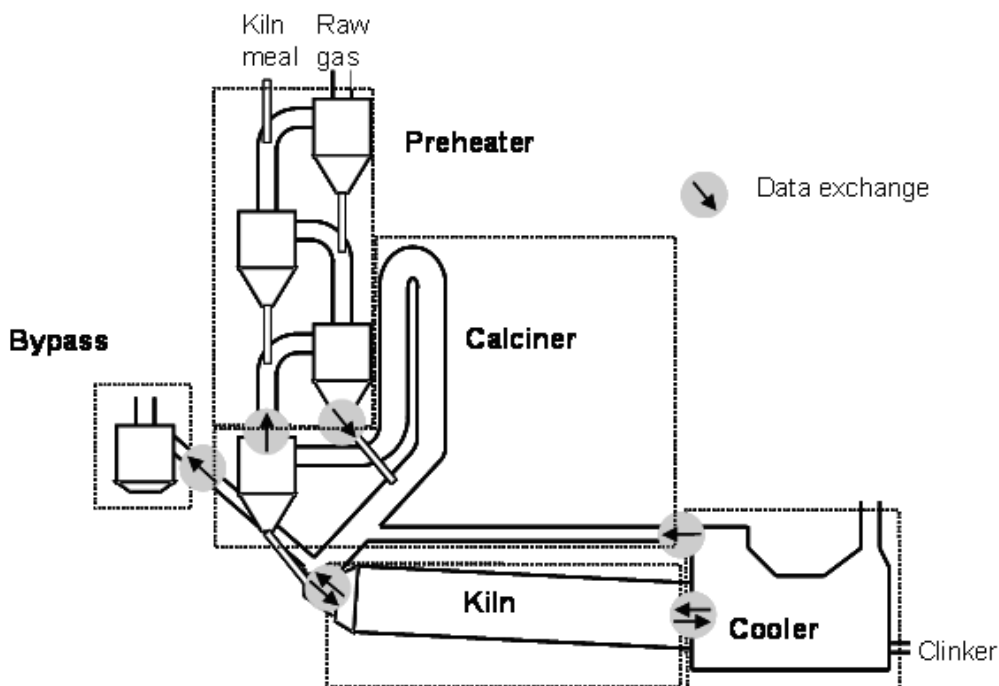
Figure 3.1 Simplified schematic of the VDZ model structure.

The gas off-take at the kiln inlet can also be defined for investigating the effect of a bypass. The calculations themselves cover the energy and material balances for the flows of fuel, dust and gas. The relevant chemical and mineralogical solid state reactions and the gas phase reactions as well as the gas-solids reactions are taken into account in addition to the combustion calculations for the fuels and heat transfer.

The result is that the calculations provide not only comprehensive process variables, such as mass and volume flows and their compositions, gas and solids temperatures and heat losses but also the specific energy requirement for burning the clinker.

3.2   Polimi model

3.2.1   Modelling approach

The mass and energy balances of the reference cement kiln have been reproduced by Polimi starting from the detailed mass balance provided by VDZ. Mass and energy balances have been estimated by the proprietary code GS [GS] developed by the GECOS group of the Department of Energy of the Politecnico di Milano. The program has the capability of simulating complex energy processes by means of a modular structure. The GS process simulation model does not include any predictive model for the calculation of the cement kiln components. Therefore, parameters such as the efficiency of cyclones, the calcination efficiency in pre-calciner, the heat losses, etc. are provided as inputs to the GS code as they result from external models or from proper assumptions. The sub-processes of the cement kiln are therefore simulated by assembling a combination of elemental components like mixers, splitters, heat exchangers and chemical reactors. A very simple example regards the simulation of the last riser-cyclone stage of the preheating tower, conceptually represented in Figure 3.2. The riser-cyclone stage is simulated by using two mixers (A, D) and two splitters (B, C). The first mixer (A - riser) receives the fresh raw meal fed to the cement kiln (stream #0) and the gaseous stream coming from the previous preheater stage (#1), and releases a gas-solid mixture at the equilibrium temperature. The components B,C and D represents the cyclone: in B, the gaseous flow (#4) is separated from the solid particles (#3), in C a fraction of the solid stream is separated from the main flow to simulate the cyclone efficiency. The uncollected stream (#5) is then mixed in the last component of the stage (D), which releases the final gas-solid mixture (#7). The remaining solid stream is sent to the following preheating stage (components E, F, G, H). In each riser-cyclone stage, the riser (components A, E, I, etc…) can be also used for simulating reactions, as for example the decomposition of $MgCO_3$ into MgO and CO_2 (@450°C); in addition, this component is also exploited to set (as an input value) the heat losses associated with the preheating stage.
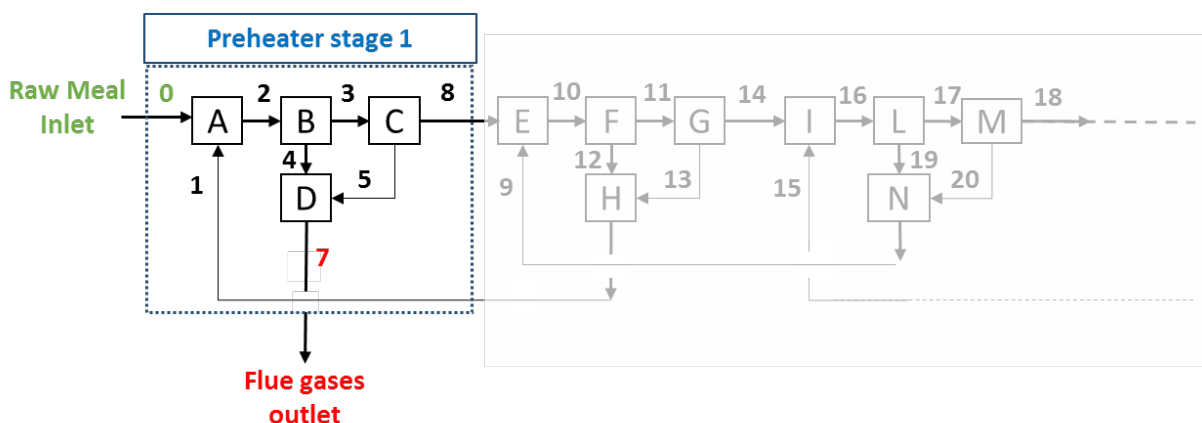

Figure 3.2: Modular structure used for simulating the first three riser-cyclone stages of the preheating tower.

Once the input file has been developed by assessing all the streams sequence and the related components layout, GS performs the iterative calculation of each component providing the overall

mass and energy balances. Although the current GS version offers the possibility of simulating complex systems with great flexibility and limited computing time, it features a simplified modelling approach:

- Chemical reaction subroutines do not contain any correlation for simulating kinetic processes or transport phenomena. For this reason, the kinetics of gas-solid reactions in the rotary kiln, in the pre-calciner and in the preheating tower are not calculated in the present model. Similarly, the gas-solid mass and heat transfer is not computed by means of mass and heat transfer coefficients. In the example shown in Figure 3.1, the heat transfer occurring in the riser (A) is calculated by assuming the temperature equilibrium between the two phases at the component outlet, whereas the wall to ambient heat transfer is simulated by setting the heat losses in the same component.
- All species are simulated by GS as ideal species (i.e. ideal gases, liquid and solids) with the exception of pure water. Mixtures are also calculated as ideal mixtures. For this reason, other codes (e.g. Aspen plus) has to be used for simulating processes where real fluid effects are non-negligible and where vapor-liquid equilibria calculations are needed (e.g. CO_2 compression and purification). For the simulation of the reference clinker burning line, the ideal gas equation of state ensures a proper accuracy of the calculations, due to the high temperature and low pressure of the process.
- Off-design simulations cannot be performed with automatic calculations. For off-design calculations, the basic assumptions used for process modelling have to be adapted based on external component modelling.
- Built-in correlations are available for the simulation of steam and gas turbines, but all the other components must be calculated by setting the most characteristic values as inputs. As an example, no correlations are available for the simulation of gas-solid separators: the collecting efficiency of cyclones must be imposed by setting the separation efficiency.

When simulating a generic process, the GS main routine calls the input and the thermodynamic properties files. The latter must include the properties of each species relevant for the process. The source format used to define thermodynamic properties reflects the shape of NASA polynomials, conceptually reported in the following equations [GAR, 1984]:

$$C_p = \frac{R}{M} (a_1 + a_2 \cdot T + a_3 \cdot T^2 + a_4 \cdot T^3 + a_5 \cdot T^4) \tag{1}$$

$$h = \frac{R}{M} \cdot \left(a_1 \cdot T + \frac{a_2}{2} \cdot T^2 + \frac{a_3}{3} \cdot T^3 + \frac{a_4}{4} \cdot T^4 + \frac{a_5}{5} \cdot T^5 + a_6 \right) \tag{2}$$

$$s = \frac{R}{M} \cdot \left(a_1 \cdot ln(T) + a_2 \cdot T + \frac{a_3}{2} \cdot T^2 + \frac{a_4}{3} \cdot T^3 + \frac{a_5}{4} \cdot T^4 + a_7 \right) \tag{3}$$

Each polynomial expression is used to calculate the specific heat (J/mol K, eq. 1) the specific enthalpy (J/mol, eq. 2) and the specific entropy (J/mol K, eq. 3) of the specie. The correlations depend on the determination of coefficients a1-a7, regressed against thermodynamic databases available in [JANAF, 1971; NASA; NIST]. Although GS contains all the modules needed for simulating the cement kiln, the solid species involved in the cement manufacturing are not present in the standard library. The thermodynamic properties of the species were hence reviewed, and a detailed bibliography and computational analysis were dedicated to complete the properties files with the missing species. Few data are available in open literature for describing clinker properties. In this work, the polynomial expression of [MAT, 2007] were used to modeling the properties of clinker species alite (C3S- 3CaO*SiO$_2$), belite (C2S-2CaO*SiO$_2$) aluminate (C3A – 3CaO*Al$_2$O$_3$) and ferrite (C4AF – 4CaO*Al$_2$O$_3$*Fe$_2$O$_3$).

It has to be remarked that some simplifying assumptions have been made with respect to the reference VDZ simulation, that does not affect significantly the quality of the final result. In particular:

- gas-solid contactors are assumed to be ideal mixers: in each preheating stage, gas and solid streams reach the equilibrium temperature at the riser outlet. Considering the temperature differences of few degrees between the solids and the gases, this assumption has a limited effect on the temperature profile along the preheating tower.
- Some chemical species present in low amount in the solids population are not considered when calculating the mass and energy balances. The species ignored are some intermediate calcium aluminates and calcium ferrites ($CaO*Al_2O_3$ and $2CaO*Fe_2O_3$) that are formed in the calciner and then remain as minor clinker constituents. In addition, all sodium, potassium and chlorine compounds are also left out from the simulation.
- The mass flow rate of SiO_2 fed to the cement plant is tuned to match the concentration ratio C3S/C2S in the clinker composition. The mass flow rates of the remaining solid species at the preheater inlet (CaO, Fe_2O_3, etc) are the same as in the reference VDZ simulation.

3.2.3   Model validation and results

In this section, a brief discussion on the mass and energy balance predicted by the GS model is reported. Furthermore, the main differences observed between the GS and VDZ simulation results are also highlighted.

In Figure 3.3, the evolution of the mass flow rate of the calcium-based species along the cement burning process is reported, including the clinker compounds. The main difference between the two models is related to the CaO mass flow rate in the calciner section, whereas the mass balances of the other main species are very similar in all the cement plant main sections. The difference in the calciner section is due to the fact that the GS model does not consider the formation of the species C2F and CA and therefore results in higher CaO mass flow rates.

GS Simulation (Ca species)

	Preheater Raw Meal In	Calciner Raw Meal In	Calciner Meal Out	Calciner Cyclone in	Calciner Cyclone out	Kiln Meal In	Kiln Clinker Hot Out	Cooler Clinker Hot In	Cooler Clinker Cold Out
CaO	0.000	5.902	24.741	24.741	18.702	18.702	0.267	0.267	0.250
CaCO3	42.971	42.014	3.287	3.287	2.485	2.485	0.000	0.000	0.000
C3S	0.000	0.538	2.259	2.259	1.708	1.708	22.447	22.447	21.065
C2S	0.000	1.798	7.537	7.537	5.697	5.697	4.888	4.888	4.587
C4AF	0.000	0.092	0.389	0.389	0.294	0.294	3.330	3.330	3.125
C3A	0.000	0.113	0.476	0.476	0.360	0.360	3.406	3.406	3.196

VDZ simulation (Ca species)

	Preheater Raw Meal In	Calciner Raw Meal In	Calciner Meal Out	Preheater Meal In	Preheater Meal Out	Kiln Meal In	Kiln Clinker Hot Out	Cooler Clinker Hot In	Cooler Clinker Cold Out
CaO	0.000	5.577	22.134	22.134	16.888	16.888	0.262	0.262	0.246
CaCO3	42.971	41.172	3.844	3.844	2.484	2.485	0.000	0.000	0.000
C3S	0.000	0.539	2.247	2.247	1.707	1.707	22.946	22.946	21.552
C2S	0.000	1.807	7.138	7.138	5.699	5.698	4.996	4.996	4.692
C4AF	0.000	0.092	0.385	0.385	0.293	0.293	3.058	3.058	2.872
C3A	0.000	0.114	0.474	0.474	0.360	0.360	3.571	3.571	3.354

Figure 3.3 Mass flow rate of the calcium-based species along the cement kiln sections in the GS and VDZ simulations. The mass flow rates are related to the main stream (dust recirculation is not included).

In Figure 3.4 the temperature profile along the suspension preheater is shown. Two lines are shown for the VDZ case, corresponding to the gas and solid phases, while just one curve is drawn for the GS model, since solids and gas exit each preheater stage at the same temperature. The agreement between the two models is good. Specific remarks can be made on the temperatures at the extremes

of the preheater. At the outlet of Stage 0, representing the outlet stream from the pre-calciner cyclone, a temperature difference of 8°C is calculated, which results from the assumed calcination efficiency of 94.2% (set equal to the calcination efficiency obtained with the VDZ model). This difference is substantially due to the missing exothermic reactions associated to the formation of the calcium compounds C2F and CA, which are neglected in the GS simulations. As for the gases at the exit of the preheating tower (Stage 4), a temperature difference of 1°C is calculated.

	Inlet	Stage 4	Stage 3	Stage 2	Stage 1	Calciner	Stage 0
--- Solid Phase-VDZ	60	296	483	640	755	868	860
—— Gas Phase - VDZ		314	498	651	764	860	860
—— Gas & Solid phase - GS	60	313	484	623	743	852	852
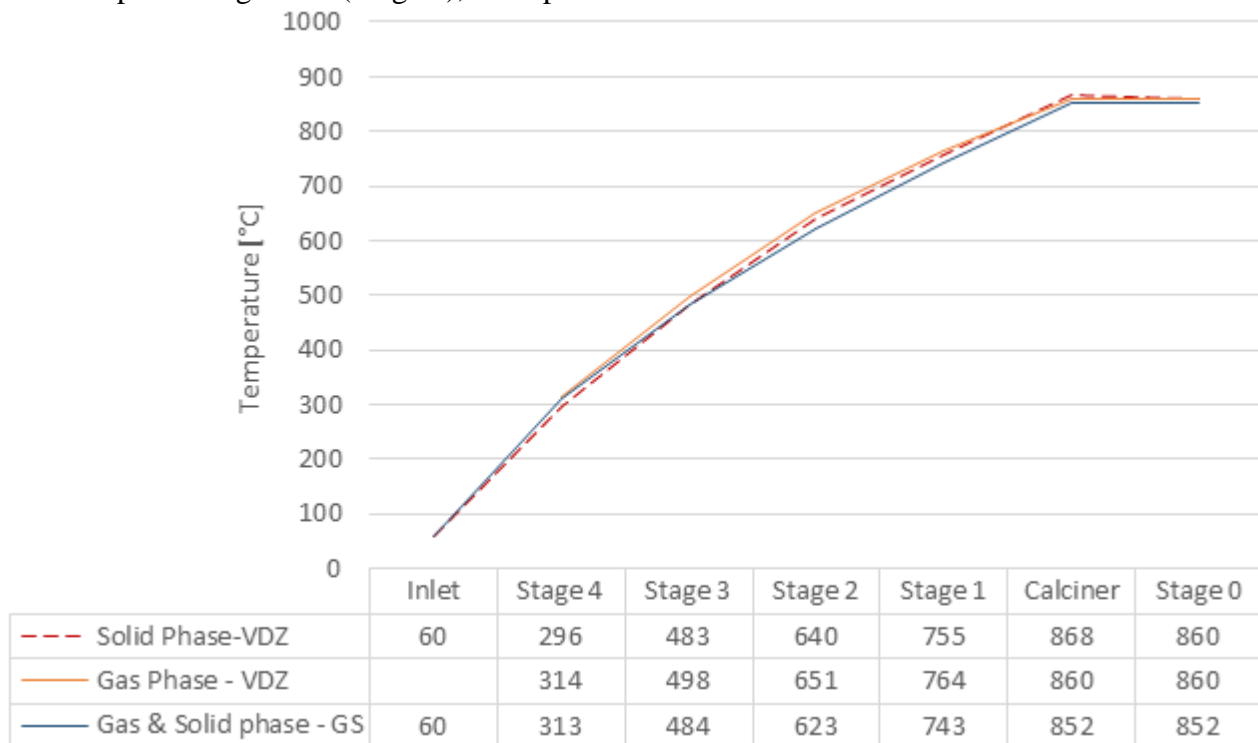
Figure 3.4 Temperature profiles along the suspension preheater.

In Table 3.2, the global results of the cement kiln balance are shown. Minor differences are obtained for the specific heat input and CO_2 emissions, which are due to the different mass flow rate of clinker resulting from the GS simulation (-2.5%). This mass balance gap is due to: (i) the species not included in the GS simulation, (ii) the criteria adopted for calculating the SiO_2 contained in the raw meal and (iii) to some small inconsistencies found in the reference VDZ balance (especially regarding the mass balance of magnesium-based species). The combination of these differences leads to higher specific energy consumption and CO_2 emissions predicted by the GS model, which are about 2% higher with respect to the reference VDZ case.

Table 3.2 Overall performances of the cement plant simulated by GS and VDZ models.

Cement plant global balance	GS	VDZ
Clinker, ton/h	117.6	120.6
Clinker, kg/s	32.68	33.51
Total fuel input, kg/s	3.87	3.87
Fuel to kiln, % of total fuel input	38.0	38.0
Total heat input, MW_{LHV}	104.47	104.47
Specific Heat Input, kJ/kg_{clk}	3197	3135
Specific CO_2 emissions, g_{CO2}/kg_{clk}	863.1	845.6

For the sake of completeness, flow rate, temperature and composition of the streams indicated in Figure 3.5 resulting from the simulation are reported in Table 3.3 and Table 3.4, as obtained with Polimi and VDZ models respectively.

CEMENT PLANT LAYOUT

Figure 3.5 Configuration of the reference cement plant.

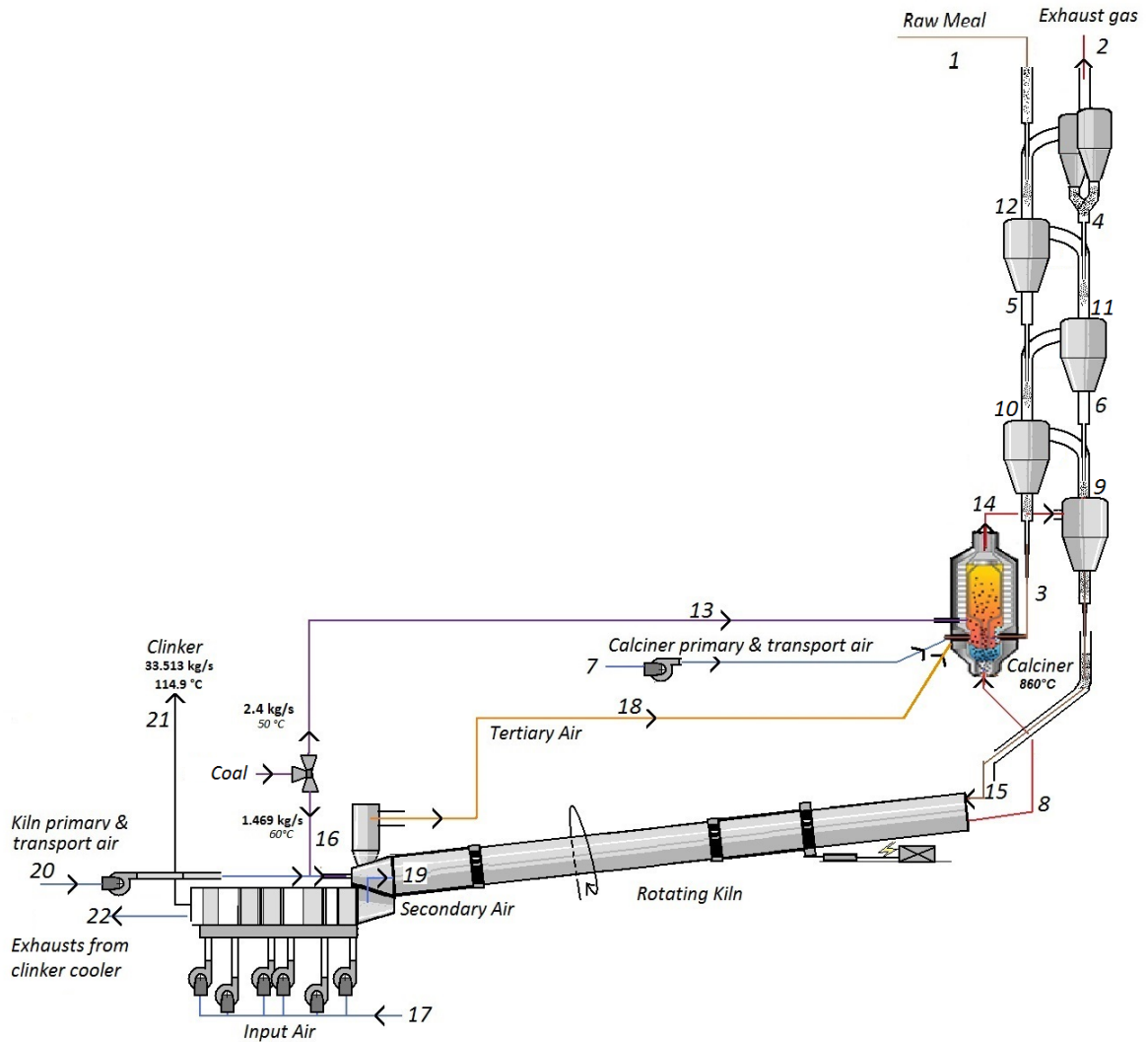| #	G, kg/s	T, °C	M, kmol/s	Ar	CO_2	H_2O	N_2	O_2	S	SO_2	$H_2O(L)$	C4AF	C3S	C3A	C2S	CaO	$CaCO_3$	SiO_2	Al_2O_3	Fe_2O_3	$MgCO_3$	MgO	$CaSO_4$
1	54.35	60.0	0.67									0.0	0.0	0.0	0.0	0.0	79.3	13.8	3.3	2.0	1.5	0.0	0.0
2g	65.9	312.5	2.01	0.7	31.9	5.1	59.0	3.3	0.0	0.0	0.0												
2s	2.6	312.5	0.03									0.0	0.0	0.0	0.0	0.0	79.3	13.8	3.3	2.0	1.5	0.0	0.0
3	63.7	742.9	0.73									0.1	0.8	0.2	2.8	9.3	66.0	14.1	3.7	2.2	0.0	0.8	0.0
4	61.6	312.5	0.67									0.0	0.0	0.0	0.0	0.0	79.3	13.8	3.3	2.0	1.5	0.0	0.0
5	61.7	484.1	0.67									0.0	0.0	0.0	0.1	0.2	79.1	13.8	3.4	2.0	1.3	0.1	0.0
6	61.9	622.7	0.68									0.0	0.1	0.0	0.4	1.4	77.9	13.9	3.4	2.1	0.0	0.7	0.0
7	0.7	15.0	0.03	0.9	0.0	1.0	77.3	20.7	0.0	0.0	0.0	0.0	0.0	0.0	0.0	0.0	0.0	0.0	0.0	0.0	0.0	0.0	0.0
8g	17.1	1078.5	0.56	0.8	19.7	6.3	71.2	1.9	0.0	0.0	0.0												
8s	2.9	1078.5	0.01									9.6	64.5	9.8	14.0	0.8	0.0	0.0	0.0	0.0	0.0	1.1	0.2
9g	63.52	852.0	1.93	0.7	33.0	4.8	58.8	2.7	0.0	0.0	0.0												
9s	12.4	852.0	0.17									0.6	3.7	0.8	12.3	40.5	5.4	12.2	4.0	2.3	0.0	0.9	0.1
10g	63.9	742.9	1.94	0.7	32.7	4.8	58.9	2.9	0.0	0.0	0.0												
10s	10.6	742.9	0.12									0.0	0.8	0.2	2.8	9.3	66.0	14.1	3.7	2.2	0.0	0.8	0.0
11g	64.6	622.7	1.96	0.7	32.7	4.8	58.8	3.0	0.0	0.0	0.0												
11s	10.1	622.7	0.11									0.0	0.0	0.0	0.4	1.4	77.9	13.9	3.4	2.1	0.0	0.7	0.0
12g	65.0	484.1	1.97	0.7	32.5	4.7	59.0	3.1	0.0	0.0	0.0												
12s	10.0	484.1	0.11									0.0	0.0	0.0	0.1	0.2	79.1	13.8	3.4	2.0	1.3	0.1	0.0
13	2.4	60.0	0.12	69% C, 4% H, 0.5%S, 0.48%N, 9%O, 16.5%Ash, 0.5%Moisture, 0.02% Cl; LHV=27 MJ/kg																			
14	63.5	852.0	1.93	0.7	33.0	4.8	58.8	2.7	0.0	0.0	0.0												
14s	50.7	852.0	0.70									0.8	4.5	0.9	14.9	48.8	6.5	14.8	4.9	2.8	0.0	1.1	0.2
15	38.3	852.0	0.53									0.8	4.5	0.9	14.9	48.8	6.5	14.8	4.9	2.8	0.0	1.1	0.2
16	1.5	60.0	0.08	69% C, 4% H, 0.5%S, 0.48%N, 9%O, 16.5%Ash, 0.5%Moisture, 0.02% Cl; LHV=27 MJ/kg																			
17	76.9	15.0	2.66	0.9	0.0	1.0	77.3	20.7	0.0	0.0	0.0												
18g	26.2	1137.0	0.91	0.9	0.0	1.0	77.3	20.7	0.0	0.0	0.0												
18s	0.7	1137.0	0.00									9.6	64.5	9.8	14.0	0.8	0.0	0.0	0.0	0.0	0.0	1.1	0.2
19g	10.8	1137.0	0.37	0.9	0.0	1.0	77.3	20.7	0.0	0.0	0.0												
19s	0.3	1137.0	0.00									9.6	64.5	9.8	14.0	0.8	0.0	0.0	0.0	0.0	0.0	1.1	0.2
20	3.4	15.0	0.12	0.9	0.0	1.0	77.3	20.7	0.0	0.0	0.0												
21	32.7	114.9	0.15									9.6	64.5	9.8	14.0	0.8	0.0	0.0	0.0	0.0	0.0	1.1	0.2
22g	39.9	284.9	1.38	0.9	0.0	1.0	77.3	20.7	0.0	0.0	0.0												
22s	1.2	787.7	0.01									9.6	64.5	9.8	14.0	0.8	0.0	0.0	0.0	0.0	0.0	1.1	0.2

Table 3.3: Thermodynamic properties of the streams shown in Figure 3.4 resulting from the GS cement plant simulation.

#	G. kg/s	T, °C	Ar	CO_2	H_2O	N_2	O_2	SO_2	$H_2O(L)$	C4AF	C3S	C3A	C2S	CaO	$CaCO_3$	SiO_2	Al_2O_3	Fe_2O_3	$MgCO_3$	MgO	$CaSO_4$
1	55.6	60.0							1.0	0.0	0.0	0.0	0.0	0.0	78.2	14.0	3.3	2.0	1.5	0.0	0.0
2g	65.7	314.4	0.0	32.0	6.2	58.8	3.0	0.0													
2s	2.6	295.8							0.0	0.0	0.0	0.0	0.0	0.0	79.0	14.1	3.3	2.0	1.5	0.0	0.0
3	64.7	755.3							0.0	0.1	0.9	0.2	2.9	9.0	66.3	14.8	2.7	1.6	1.3	0.2	0.0
4	62.6	295.8							0.0	0.0	0.0	0.0	0.0	0.0	79.0	14.1	3.3	2.0	1.5	0.0	0.0
5	62.7	482.9							0.0	0.0	0.0	0.0	0.1	0.2	78.7	14.1	3.3	2.0	1.5	0.0	0.0
6	62.9	639.5							0.0	0.0	0.1	0.0	0.5	1.5	77.0	14.2	3.2	1.9	1.5	0.0	0.0
7	0.7	15.0	0.0	0.0	1.0	78.0	21.0	0.0													
8g	17.1	1078.5	0.0	20.4	6.5	71.5	1.5	0.1													
8s	2.9	1103.5							0.0	8.4	45.3	10.4	27.9	4.3	0.0	2.8	0.8	0.1	0.0	0.1	0.0
9g	62.9	859.9	0.0	33.2	4.9	59.2	2.8	0.0													
9s	12.6	860.1							0.0	0.9	5.1	1.1	16.9	50.1	7.4	17.4	0.0	0.0	0.1	1.0	0.1
10g	63.5	763.9	0.0	33.2	4.8	59.2	2.8	0.0													
10s	10.6	755.3							0.0	0.1	0.9	0.2	2.9	9.0	66.3	14.8	2.7	1.6	1.3	0.2	0.0
11g	64.0	651.1	0.0	33.1	4.8	59.3	2.7	0.0													
11s	10.2	639.5							0.0	0.0	0.1	0.0	0.5	1.5	77.0	14.2	3.2	1.9	1.5	0.0	0.0
12g	64.3	498.0	0.0	32.9	4.8	59.5	2.8	0.0													
12s	10.2	482.9							0.0	0.0	0.0	0.0	0.1	0.2	78.7	14.1	3.3	2.0	1.5	0.0	0.0
13	2.4	60.0	69% C, 4% H, 0.5%S, 0.48%N, 9%O, 16.5%Ash, 0.5%Moisture, 0.02% Cl; LHV=27 MJ/kg																		
14g	62.4	871.1	0.0	33.2	4.9	59.3	2.7	0.0													
14s	52.6	868.1							0.0	0.9	5.0	1.1	16.0	49.6	8.6	17.6	0.1	0.0	0.2	1.0	0.1
15	39.8	860.1							0.0	0.9	5.1	1.1	16.9	50.1	7.4	17.4	0.0	0.0	0.1	1.0	0.1
16	1.5	60.0	69% C, 4% H, 0.5%S, 0.48%N, 9%O, 16.5%Ash, 0.5%Moisture, 0.02% Cl; LHV=27 MJ/kg																		
17	82.8	15.0	0.0	0.0	1.0	78.0	21.0	0.0													
18g	26.2	1049.8	0.0	0.0	1.0	78.0	21.0	0.0													
18s	0.7	1085.6							0.0	8.8	65.8	10.2	14.3	0.8	0.0	0.0	0.0	0.0	0.0	0.0	0.0

Table continues in the next page

#	G. kg/s	T, °C	Ar	CO_2	H_2O	N_2	O_2	SO_2	$H_2O(L)$	C4AF	C3S	C3A	C2S	CaO	$CaCO_3$	SiO_2	Al_2O_3	Fe_2O_3	$MgCO_3$	MgO	$CaSO_4$
19g	10.4	1136.9	0.0	0.0	1.0	78.0	21.0	0.0													
19s	0.3	1136.9							0.0	8.8	65.8	10.2	14.3	0.8	0.0	0.0	0.0	0.0	0.0	0.0	0.0
20	3.3	15.0	0.0	0.0	1.0	78.0	21.0	0.0													
21	33.5	114.9							0.0	8.8	65.8	10.2	14.3	0.8	0.000	0.0	0.0	0.0	0.0	0.0	0.0
22g	46.2	284.9	0.0	0.0	1.0	78.0	21.0	0.0													
22s	1.2	284.9							0.0	8.8	65.8	10.2	14.3	0.8	0.0	0.0	0.0	0.0	0.0	0.0	0.0

Table 3.4 Thermodynamic properties of the streams shown in Figure 3.5 resulting from the VDZ cement plant simulation.

4 ELECTRICITY CONSUMPTIONS

With a total consumption of 97 kWh per ton of cement, electricity represents one of the main contributions in determining the final cost of cement. Most of the electricity consumptions are normally associated to milling and handling of solids and are constant when different capture technologies are considered. However, electric consumption associated with fans and fuel milling and handling will depend on the specific capture technology considered, since it will influence the flow rate and pressure losses of gas flows and fuel consumptions. Therefore, for a complete comparison of capture technologies, the electric consumptions associated to these units have to be calculated.

Table 4.1 shows the electric consumption of the reference cement plant putting in evidence the main fans of the burning line and the coal handling and milling line consumptions, because these contributions will be subject to variations in the CO_2 capture configurations. Electric consumptions of fans are calculated from the volume flow rate (calculated from the mass balances and the assumed false air leakages under the "typical air leak" conditions specified in the CEMCAP framework document D3.2), the pressure rise (taken from common practice) and by assuming a total efficiency of 75% for all fans. For coal milling and handling, a specific electric consumption of 53.6 kWh/t_{coal} is considered. All the other auxiliaries consumption (related to electric drives, milling and handling of solids, etc.) are calculated by difference, considering the total assumed consumption of 97 kWh per ton of cement.

Table 4.1 Electric consumptions associated to cement plant auxiliaries. The position and the names of the fans are indicated in Figure 4.1.

FANS	Flow rate, m³/h	Flow rate, Nm³/h	Temp., °C	Δp, daPa	Power, kWe	Power kWhel/tcem
ID fan	349440	162564	314	635	822	4.72
Raw Mill fan	411712	293512	110	1070	1632	9.36
Filter Fan	584117	439355	90	180	389	2.23
Cooler Fans	245081	232323	15	215	195	1.12
Coal milling and handling	-	-	-	-	747	4.28
Others (by difference)*	-	-	-	-	13121	75.28
Total	-	-	-	-	16906	97

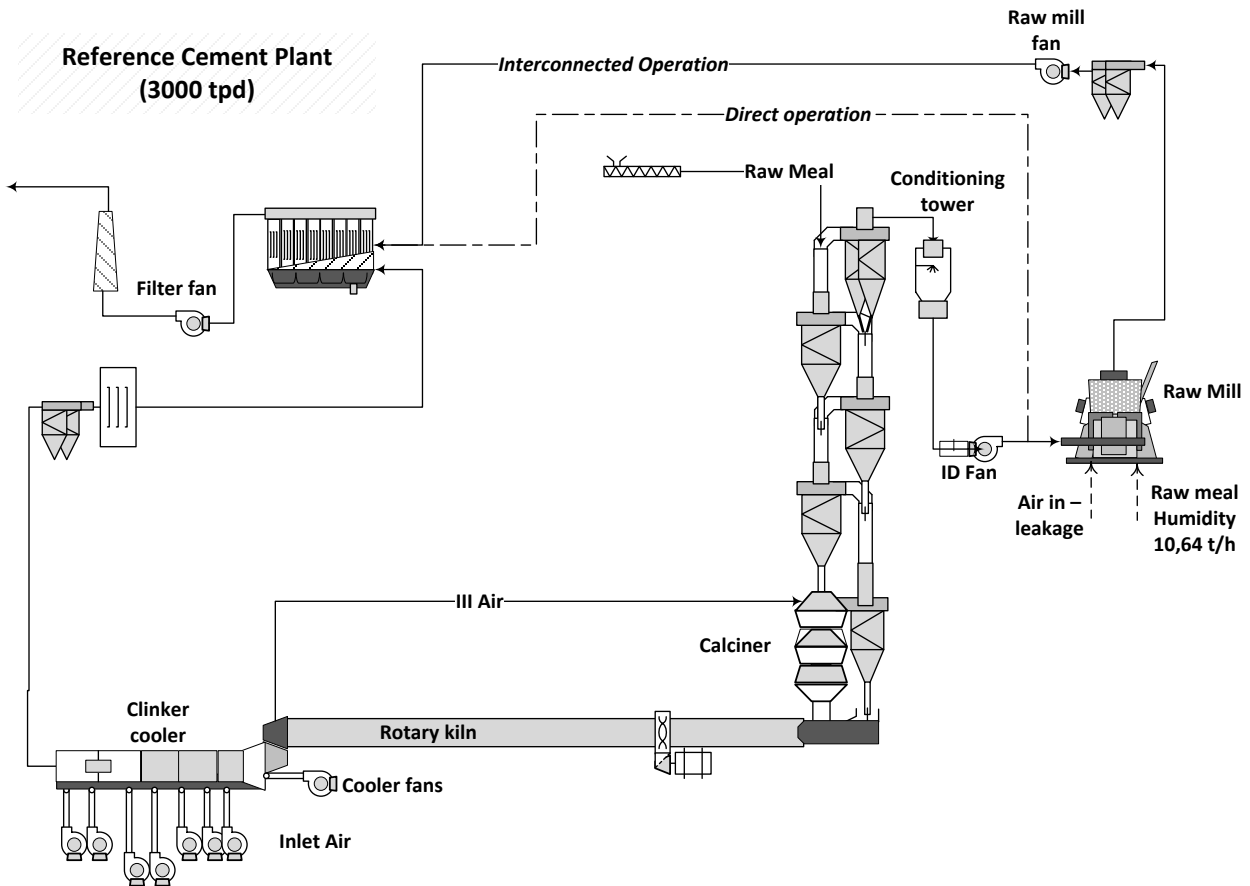** includes raw meal and cement grinding, solids handling, kiln drive, lighting, etc.*

Figure 4.1 Schematic of the burning line, indicating the position and the names of the fans. "Direct operation" configuration is adopted a few hours per day.

5 ECONOMIC ANALYSIS OF THE REFERENCE CEMENT PLANT WITHOUT CO₂ CAPTURE

The economic analysis is based on the methodology and assumptions described in CEMCAP deliverable 3.2. Assumptions are reported in Table 5.1.

Table 5.1 Main assumptions for the economic analysis.

FINANCIAL ASSUMPTIONS	
Capacity factor , %	91.3
Tax rate, %	0
Operational life, years	25
Construction time, years	2
Inflation rate, %	0
Discounted cash flow rate, %	8
CAPEX	
Total direct costs (TDC), M€2014 *	148.8
Engineering, procurement, construction (EPC)	TDC*1.14
Total plant cost (TPC)	EPC*1.15
OPEX	
Raw meal, €/t_{clk}	5
Fuel price, €/GJ_{LHV}	3
Price of electricity, €/MWh_{el}	58.1
Carbon tax, €/t_{CO2}	0
Other variable O&M, €/t_{cement}	0.8
Insurance and loc. Tax, % TPC	2
Maintenance cost (including maintenance labor), % TPC	2.5
Cost of labor per person – k€/year	60
Operating labor - N° of persons	100
Maintenance labor cost, % Maintenance	40
Administrative labor cost, % O&M labor	30

Base TDC cost = 145.5 M€ from [IEAGHG, 2013], corrected with CEPCI index 2013->2014 = 1.023 [CHEMENG, 2016]

A total cost of cement of 44.6 €/t_{cement} has been calculated. It has to be highlighted that this value does not include the contribution of freights, transport, re-naturation of quarries etc. The share of the different contributors to the cement cost is reported in Table 5.2. The total cost calculated in this work is lower than the 51.4 €/t_{cement} reported in [IEAGHG, 2013]. The main reasons for this difference are due to the higher capacity factor assumed in CEMCAP (91.3%, vs. 80%), causing a higher impact of Capex and fixed Opex, and to the lower price of electricity assumed in CEMCAP (58.1 €/MWh vs. 80 €/MWh).

In Figure 5.1, a sensitivity analysis on fuel price, electricity price and carbon tax is reported. A variation of the fuel and electricity prices by +/−50% causes a variation of the cement cost of 6.0-7.7%. The introduction of a carbon tax of 50 €/t_{CO2} would lead to an increase of the cost of cement to 75.7 €/t (+70%).

Table 5.2 Economic results: operating, fixed and capital costs associated to the baseline cement plant.

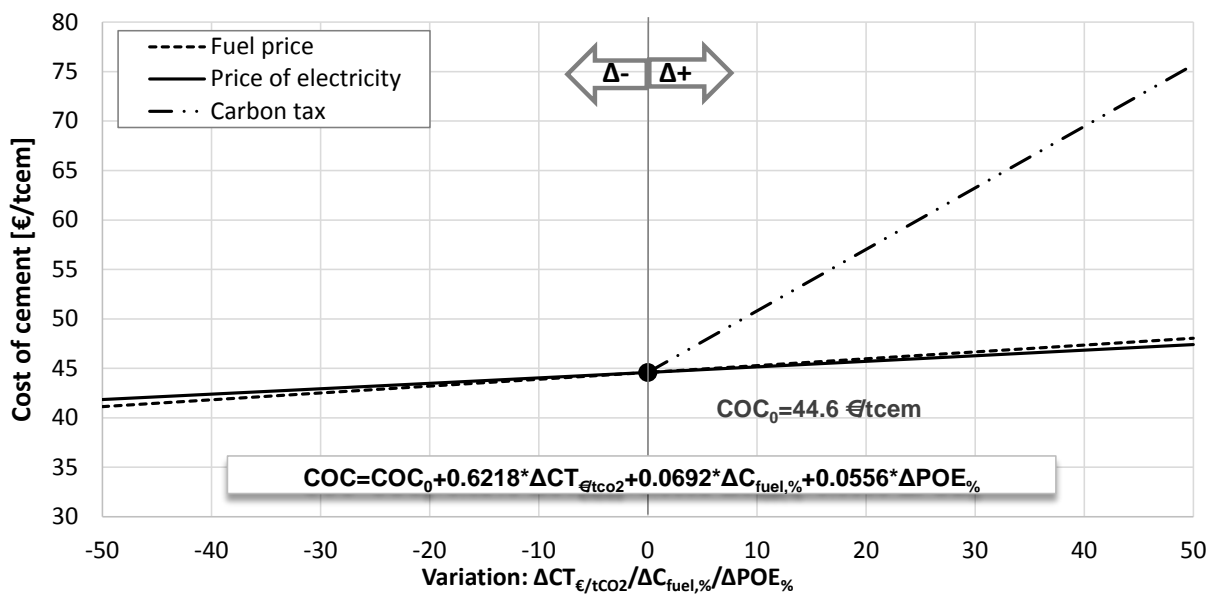| RESULTS – Cost of cement (COC)	[€/t$_{cement}$]
Raw meal	5.00
Fuel	9.41
Electricity	7.66
Carbon tax	-
Other variable costs	1.09
Variable Opex	**23.16**
Operative, administrative and support labor	8.69
Insurance and local taxes	4.04
Maintenance cost (including maintenance labor)	5.05
Fixed Opex	**17.79**
Capex	**19.70**
Cost of cement	**44.6**

Figure 5.1 Influence of fuel/electricity price and carbon tax on the cost of cement. The sensitivity analysis considers a variation of ±50% with respect to the reference fuel and electricity prices, and a variation 0-50 €/t$_{CO2}$ for the carbon tax.

REFERENCES

[BREF, 2013]   JRC Reference Reports - Best Available Techniques (BAT) Reference Document for the Production of Cement Lime and Magnesium Oxide. European Commission, 2013

[CHEMENG, 2016]   www.chemengonline.com

[ECRA]   www.ecra-online.org/226/

[GS]   Gecos, GS software. http://www.gecos.polimi.it/software/gs.php

[GAR, 1984]   Gardiner WC, editor, 1984. Combustion chemistry. New York (NY, USA): Springer-Verlag.

[IEAGHG, 2013]   IEAGHG, 2013. Deployment of CCS in the cement industry. Report 2013/19.

[JANAF, 1971]   Stull DR, Prophet H., 1971. JANAF thermochemical tables. 2nd ed. Washington, DC (USA): US National Bureau of Standards.

[NASA]   http://www.grc.nasa.gov/WWW/CEAWeb/ceaThermoBuild.htm

[NIST]   NIST DATABASE, www.webbok.nist.gov/chemistry/

[MAT, 2007]   T. Matschei, B. Lothenbach, and F. P. Glasser, 2007. Thermodynamic properties of Portland cement hydrates in the system $CaO–Al_2O_3–SiO_2–CaSO_4–CaCO_3–H_2O$. Cem. Concr. Res., 37, 1379–1410.